Environmental Research 286 (2025) 122740

Contents lists available at ScienceDirect

Environmental Research

journal homepage: www.elsevier.com/locate/envres

Retention of increased maximum oxyregulation capacity in corals transplanted from an extreme mangrove environment to a reef flat

Nicole J. Dilernia [a,*], David J. Suggett [a,b], Christine D. Roper [a], Rachel Alderdice [c], Christian R. Voolstra [c], Michael Kühl [d], Emma F. Camp [a]

[a] Climate Change Cluster, University of Technology Sydney, Ultimo, 007, NSW, Australia
[b] KAUST Coral Restoration Initiative (KCRI) and Division of Biological and Environmental Science and Engineering (BESE), King Abdullah University of Science and Technology, Thuwal, 23955, Saudi Arabia
[c] Department of Biology, University of Konstanz, 78464, Konstanz, Germany
[d] Department of Biology, Marine Biological Section, University of Copenhagen, Strandpromenaden 5, 3000, Helsingør, Denmark

ARTICLE INFO

Keywords:
Hypoxia-inducible factor
Hypoxia response curves
Ocean deoxygenation
Oxyregulator
Pocillopora acuta, Transcriptomics

ABSTRACT

Loss of oxygen (O_2) from the world's oceans to physiologically-critical levels ("hypoxia") is an important, yet understudied stressor for coral reefs. However, extreme reef-neighbouring ecosystems such as mangrove lagoons that are routinely subjected to frequent low-pO_2 exposure (i.e., low partial pressure of O_2), high temperature fluctuations, and low-pH, may be harbouring corals with a higher capacity for oxyregulation, rendering them more resilient to adapt to life in low-pO_2 surroundings. We investigated differences in the hypoxic response of the common reef-building coral *Pocillopora acuta* following 1-year transplantation between Low Isles reef flat (a comparatively more stable O_2 environment) and Woody Island mangrove lagoon (a more variable and oftentimes low-pO_2 habitat), on the Great Barrier Reef. Analysing hypoxia response curves and metabolic function and physiology, we found that mangrove *P. acuta* retained attributes for hypoxic tolerance when transferred between habitats. These corals survived frequent low-pO_2 exposure (<1.77 mg O_2 L^{-1}), and although total positive regulation (T_{pos}) was similar between all coral populations, mangrove-to-reef transplants exerted their maximum regulation capacity (P_{cmax}) at a lower pO_2 than all other groups, even after 1-year in a more typical O_2 environment. Gene expression analyses also revealed activation of non-hypoxia inducible factor target pathways in mangrove corals as an alternative means of anaerobic respiration. The ability of coral populations from extreme ecosystems to exert maximum regulation capacity at low-pO_2 may therefore be a long-term conserved property, based on greater O_2 metabolisation, highlighting tolerance of mangrove *P. acuta* to survive extreme O_2 conditions in this mangrove environment.

1. Introduction

Anthropogenic pressures are driving ocean deoxygenation to critical levels affecting important coastal and oceanic ecosystems. Besides driving coral bleaching outcomes (Hoegh-Guldberg, 2011), ocean warming is accelerating the physical loss of soluble oxygen (O_2) via increased water column stratification and O_2 demand (Keeling et al., 2010; Levin, 2018) deteriorating water quality in aquatic habitats (Leiva et al., 2018; Levin and Breitburg, 2015). Coral reef ecosystems are particularly at risk from deoxygenation events (Altieri et al., 2021; Hughes et al., 2020). By 2100, corals are expected to experience up to a 30 % increase in severe exposure to "hypoxia" (Pezner et al., 2023), i.e., critical O_2 levels below which a normal physiological state can no longer be supported (Johnson et al., 2024; Solaini et al., 2010). The tolerance to acute and chronic hypoxia appears to vary widely between coral taxa (e.g., Nelson and Altieri, 2019; Hughes et al., 2020; Alderdice et al., 2021; Johnson et al., 2021; Alva García et al., 2022), and in part reflects different capacities to oxy-regulate under declining O_2 conditions (Dilernia et al., 2024; Hughes et al., 2022). However, the full extent to which coral taxa can withstand deoxygenation exposure remains unclear, and in particular the capacity to acquire and retain greater tolerance to conditions that are considered hypoxic (<2 mg L^{-1}) (Deleja et al., 2022; Haas et al., 2014; Hughes et al., 2022; Johnson et al., 2021).

Reef-neighbouring ecosystems such as mangrove lagoons are

* Corresponding author.
E-mail address: Nicole.J.Dilernia@student.uts.edu.au (N.J. Dilernia).

https://doi.org/10.1016/j.envres.2025.122740
Received 4 December 2024; Received in revised form 31 July 2025; Accepted 31 August 2025
Available online 1 September 2025

naturally subjected to frequent low-pO_2 exposure (i.e., low partial pressure of O_2), due to enhanced trapping of organic matter and reduced water exchange intensifying O_2 drawdown (Altieri et al., 2021; Camp et al., 2016, 2018; Scucchia et al., 2023), as well as strong temperature and pH dynamics (Camp et al., 2016; Haydon et al., 2021) that can reach values projected under future climate change scenarios (e.g., for the year 2100; IPCC et al., 2023). Recent studies on the Great Barrier Reef (GBR), using the Woody Island mangrove lagoon as a model extreme habitat, have shown that coral populations persisting in sub-optimal seawater conditions exhibit greater resilience to stressors, e.g., via increased physiological plasticity (Camp et al., 2019; Haydon et al., 2021, 2023; Ros et al., 2021). Such corals appear to have adapted to the more extreme mangrove lagoon conditions via i) a preferential switch to heterotrophy, including a trade-off between increased respiration rates and reduced net photosynthesis (Camp et al., 2019), ii) shifts in coral microbiome composition with a greater diversity and richness in bacterial communities (Haydon et al., 2021), and iii) expression of unique coral elementomes (Camp et al., 2025). Prior work by Haydon et al. (2023) also revealed that corals from Woody Isles had higher bleaching resistance than corals from Low Isles when exposed to a laboratory heat stress experiment. Interestingly, previous transplantation studies of *P. acuta* between the Woody Island mangroves and neighbouring Low Isles reef flat have shown retention of thermal tolerance in *P. acuta* mangrove populations (up to 37.6 °C) when moved from mangrove-to-reef (Roper et al., 2025). Whether the capacity of specific tolerance to low oxygen conditions is retained in the extreme corals of the GBR mangrove lagoons remains to be examined.

In this study, we hypothesised that reef-neighbouring extreme habitats harbour corals that could exhibit a higher capacity for oxyregulation – a beneficial trait to survive low-pO_2 seawater conditions (Alderdice et al., 2021; Breitburg et al., 2018; Pezner et al., 2023) – with the aim to understand whether retention of hypoxic tolerance traits are evidence of a fixed response to surviving in an extreme coral habitat. We therefore investigated the hypoxia response of the tropical coral *P. acuta*, transplanted 1-year prior between the Low Isles reef flat (a comparatively more stable environmental system), and Woody Island mangrove lagoon (routinely subjected to low-pO_2 conditions conventionally considered hypoxic) on the GBR. Coral hypoxia tolerance capacity was determined using hypoxia response curves (HRCs) (or performance curves) – an assay historically used to parameterise the response of aquatic organisms under declining O_2 (Cobbs and Alexander, 2018; De Mutsert et al., 2015; Tremblay et al., 2020; Zhang et al., 2021) – of both native and transplanted coral populations in these two habitats, where we explored which attributes for hypoxia tolerance were retained in translocated corals. Furthermore, we determined additional metrics of coral metabolic function and physiology such as respiration rates relative to gross photosynthesis, as well as coral gene transcription, to investigate mechanisms contributing to differences in the hypoxia response of the *P. acuta* populations. We specifically hypothesised that *P. acuta* from the mangrove lagoons would exhibit greater capacity for oxyregulation and a lower hypoxic threshold relative to populations originating from the adjoining reef, where O_2 availability remains comparatively high.

2. Materials and methods

2.1. Site details and coral fragment collection

Field work was carried out in the Low Isles reef system (~16.388° S, 145.566° E) on the GBR, (Australia), ~15 km from the mainland, with all data collected between 19th – February 24, 2023. Woody Island mangrove lagoon (WIML) is characterised as a vegetative mangrove system, routinely subjected to more extreme temperature variations (>7 °C) than on the adjoining Low Isles reef flat (LIRF), as well as lower O_2 concentrations (<1 mg L^{-1}) and low pH (<7.5 pH) (Camp et al., 2019; Haydon et al., 2021). Light intensity between sites are similar, with generally only ~5 % higher photon irradiance (PAR; 400–700 nm) recorded in the mangrove lagoons than on reef flat (Camp et al., 2019; Ros et al., 2021). Additionally, prior genotyping work in Oct 2022 revealed two distinct populations of *P. acuta* between the two sites, with strong genetic variation between the two lineages (Duijser et al., 2025). ITS2 profiling has also revealed that each lineage associates with different genera of Symbiodiniaceae. Predominantly, the reef population associates with *Cladocopium*, whilst the mangrove *P. acuta* corals are mostly associated with the genus *Durusdinium* (Camp et al., 2019; Duijser et al., 2025; Ros et al., 2021).

One year prior to this study, colonies of the sub-tropical coral *P. acuta* (Lamarck, 1816) had been reciprocally transplanted between WIML and LIRF attached to aluminium racks using cable ties, which also held corals from other genera that were not included in this work (see Fig. 1b). However, an unprecedented heavy rainfall event one month prior to sampling for this study caused reduced salinity in the northern bay of the mangrove lagoon where the transplanted corals had been (Fig. 1a(i)) (Bartels et al., 2023). Therefore, as none of the existing "reef-mangrove" or "mangrove-mangrove" transplants could be used due to evidence of freshwater bleaching, additional *P. acuta* in the southern channel of the lagoon (Fig. 1a(ii)) which were unaffected by this event – likely due to a greater influence from the open ocean currents (Bartels et al., 2023) – were selected instead. The four transplant groups targeted were therefore: (i) mangrove-reef (M-R), (ii) wild mangrove (WM), (iii) reef-reef (R-R), and (iv) wild reef (WR).

In both WIML and LIRF, six native colonies of *P. acuta* were randomly selected at a depth of ca. 1.5 m, each at least 5 m apart. Coral fragments (ca. 5–10 cm length) were collected via SCUBA using wire cutters, and placed into Ziplock bags for immediate transport back to the surface support research vessel (Wavelength Reef Cruises). In addition, on LIRF, M-R transplants ($n = 6$) and R-R transplants ($n = 6$) were collected from the transplantation racks in the same manner as the native fragments (see Table 1 for full sampling index). Each fragment was further divided into two, one for photosynthesis-to-respiration (P:R) incubations, and one for recording of hypoxia response curves (HRCs), in order to compare net O_2 exchange rates and oxyregulatory capacity of transplanted corals (M-R and R-R), with origin population controls (WM and WR). All fragments were inspected and cleared of additional debris prior to any incubation.

To query differential expression of genes previously implicated in coral hypoxic stress response (e.g., Alderdice et al., 2021), we took advantage of an available RNA-Seq dataset from an upcoming study that analysed coral thermotolerance following the same 1-year translocation experiment between WIML and LIRF (Roper et al., 2025). Briefly, for sampling context, the thermal tolerance of eight fragments from each group (except for WR, $n = 7$ due to sampling limitations; Table 1) were tested over 18 h via CBASS acute heat stress assays (*sensu* Voolstra et al., 2020; Evensen et al., 2023), at experimental temperatures 30, 33, 36 and 39 °C (for full thermal ramping details, please see (Roper et al., 2025). Following the final experimental temperature ramp-down, the corals were removed from experimental tanks and immediately flash frozen for RNA sequencing analysis. The dataset was comprised of $n = 33{,}730$ genes, and differential expression was determined for comparisons between each group (M-R, WM, R-R, WR), across each experimental temperature. For expression of hypoxia response pathway genes of interest (GOI) (described below), only samples held at the baseline temperature (30 °C) were interpreted from the RNA-Seq dataset.

2.2. Abiotic characterization

Two *in situ* O_2 loggers were deployed at each study site (WIML and LIRF). Robust O_2 probes (OXROB10-SUB, PyroScience, Germany) were attached to the SUB-connector optical port of each data logger (AquapHOx-L-O2, PyroScience GmbH, Germany) and positioned at relevant coral depth (attached to the transplantation frames where applicable). The sensors were cable-tied in position, while the main bodies of the

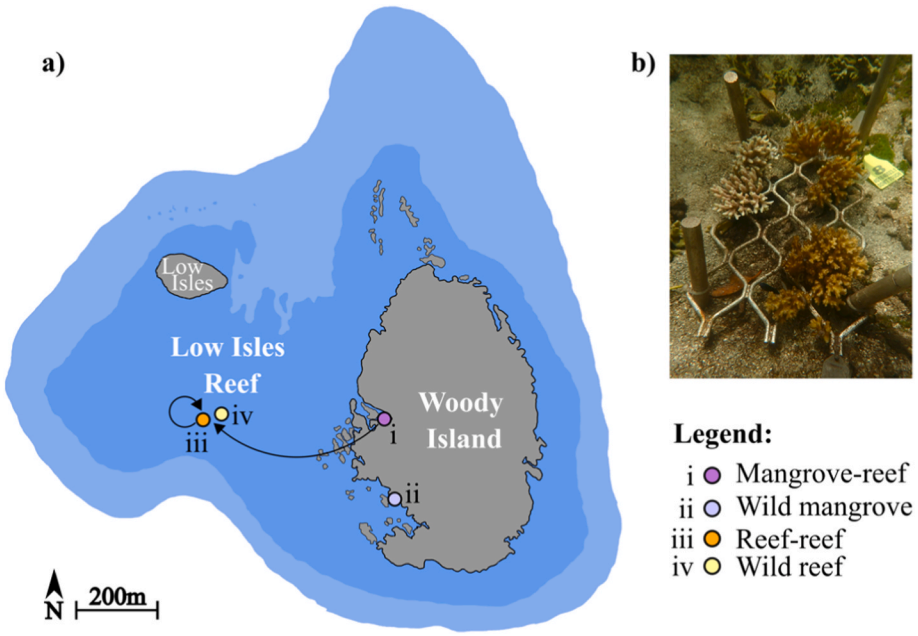

Fig. 1. a) map of the study site for Woody Island mangrove lagoon (WIML), and Low Isles reef flat (LIRF) (16.388° S, 145.566° E) on the Great Barrier Reef, Australia, with 1-year transplanted *Pocillopora acuta* groups ($n = 6$), including (i) mangrove-reef (M–R), (ii) wild mangrove (WM), (iii) reef-reef (R–R), and (iv) wild reef (WR). Coloured dots and arrows denote groups. **b)** An image of the targeted *P. acuta* transplants (and other untargeted corals e.g., *Acropora* sp.) attached to an aluminium transplantation rack, taken Feb 19, 2023 (*P.C. Emma F. Camp*).

Table 1
Sampling index for *Pocillopora acuta* coral fragments collected from Woody Island mangrove lagoon (WIML) and Low Isles reef flat (LIRF), for P:R Incubations, and hypoxia response curves (HRCs), as well as additional RNA-Seq analysis for expression of hypoxia genes of interest (GOI). Table includes sample ID, date and number of samples collected per analysis, origin of the coral population, location of the corals during sampling (between 2nd-24th February 2023), and coral specimen type (wild control sample or transplanted coral). NB: $n = 6$ to 8 per experimental analysis.

ID	Date	No. of samples	Origin	Sample	Specimen
i	22nd Feb 23 2nd Feb 23	$n = 6$ HRCs $n = 6$ P:R $n = 8$ GOI	Mangrove	LIRF	Transplanted mangrove-reef (M-R)
ii	20th Feb 23 2nd Feb 23	$n = 6$ HRCs $n = 6$ P:R $n = 8$ GOI	Mangrove	WIML	Wild mangrove (WM)
iii	19th Feb 23 24th Feb 23 2nd Feb 23	$n = 6$ HRCs $n = 6$ P:R $n = 8$ GOI	Reef	WIML	Transplanted reef-reef (R-R)
iv	21st Feb 23 2nd Feb 23	$n = 6$ HRCs $n = 6$ P:R $n = 7$ GOI	Reef	LIRF	Wild reef (WR)

loggers were secured to lead diving weights. Ambient dissolved oxygen levels (DO, mg O_2 L^{-1}) and seawater temperature (°C) were monitored (measuring at 60 s intervals) for the duration of the field sampling. The AquapHOx-L-O2 loggers were calibrated against 100 % air-saturated seawater and a 0 % Na_2SO_3 solution prior to deployment. Welch's T-tests (assuming unequal variance) with Cohen's d effect size were carried out in RStudio version 4.1.0, Build 421 (R Core Team, 2021), using installed package "rstatix" version 0.7.2 (Kassambara, 2023a) to evaluate differences in the means of the environmental O_2 conditions and temperature between WIML and LIRF. Additionally, histograms displaying the accumulative time spent (%) at each DO level and temperature (as per Camp et al., 2017) were used for inter-site comparisons.

2.3. P:R incubations (experiment 1)

Following fragmentation, corals ($n = 6$ per incubation, as outlined in Table 1) were immediately moved to a 10 L tub of fresh seawater collected from the respective sites. The holding tub was housed onboard the research vessel, aerated with a submersible water pump (Aqua One Maxi Water Pump 102, PUMAQU102), and maintained at 29 ± 0.5 °C by a 150 W bar heater (Aqua One Submersible Glass Heater, 230 V/50 Hz) for ~15 min, to match the *in situ* temperature (see Section 3.1 for environmental logger data). Each fragment was secured in a cylindrical, clear acrylic purpose-made chamber (475 mL), held by expandable plastic rings to allow space beneath for free-rotation of one 4 × 0.5 cm magnetic stir bar per chamber (PTFE, ROWE Scientific Pty Ltd). Chambers were placed inside a purpose-made acrylic incubation frame with magnetic rotation capacity for each chamber, powered by two rechargeable 12 V High Rate UPS batteries (9Ah 48W/Cell, 12SB45WHR, Drypower©). The entire incubation frame and sealed, air-tight chambers (with additional $n = 1$ blank seawater control per run) were ¾ submerged in a water bath, also maintained at 29 ± 0.5 °C by a 150 W bar heater. Temperature of the water bath was constantly monitored using an optical temperature sensor connected to an O_2 data meter (FireSting-O2, PyroScience GmbH, Germany).

Blackout cloth was used for dark incubations (<5 μmol photons m^{-2} s^{-1}), with an initial O_2 concentration measurement (μmol O_2 L^{-1}) from each chamber using a robust oxygen probe (OXROB10-SUB, PyroScience, Germany) connected to the FireSting-O2. Another O_2 measurement was taken after 1.5 h, before starting the light incubation under a photon irradiance of ~600 μmol photons m^{-2} s^{-1}; 400–700 nm), delivered via a Hydra® 64HD LED Light (Aqua Illumination, Aperture, LLC). The chosen light level was ~2–3 times higher than the saturating photon irradiance, E_k, which was determined to ~240 μmol photons m^{-2} s^{-1} via rapid light curve measurements for all corals using a Diving-PAM fluorometer (Walz GmbH, Germany), ensuring measurements of

O_2-production under saturating light conditions (Suggett et al., 2022). Photon irradiance (400–700 nm) was monitored using a miniature irradiance sensor (MQS-B Mini Quantum Sensor, Heinz Walz GmbH, Effeltrich, Germany) connected to alight meter (LI-250A; LI-COR© Bioscience, Lincoln, USA). Final O_2 concentration (μmol O_2 L^{-1}) was measured from each chamber after 1.5 h light incubation, before termination of the experiment. Prior to use, robust oxygen probes were calibrated via measurements in 100 % air-saturated seawater and a 0 % O_2 solution of Na_2SO_3 following the manufacturers procedures.

Net photosynthesis (P_N) and respiration (R) rates were determined by calculated changes in O_2 concentration during dark and light incubations, whereas gross photosynthesis (P_G) was determined by the addition of P_N and R (e.g., Camp et al., 2019). All rates were corrected for incubation volume and seawater controls to account for microbial respiration, as well as coral surface area, which was determined using the single paraffin-wax dipping method (Veal et al., 2010) (see Fig. S1 and Table S1 for coral surface area calculations). One-way ANOVAs with *post-hoc* Tukey HSD, and additional pairwise comparisons with Benjamini–Hochberg (BH) adjustments, were conducted using the RStudio package "dplyr" (Wickham et al., 2023) to compare differences in physiological parameters between sites (WIML and LIRF). Tests of homogeneity of variance (Levene's test) and normality (Shapiro-Wilk and Q-Q plots) were passed.

2.4. Hypoxia response curves (HRCs) (experiment 2)

Following fragmentation, corals were transported (~60 min) in fresh seawater collected from sampling sites, in an insulated 40 L cooler box onboard the research vessel back to a provisional laboratory setup onshore. The seawater was aerated during transfer with air-stones connected to battery-operated air pumps (Aqua One Battery Air 250), maintaining O_2 levels at > 90 % air saturation and a temperature of 29 ± 0.5 °C, as monitored using a FireSting®-GO2 (Pocket Oxygen Meter, PyroScience GmbH, Germany). Measurements of the maximum photochemical efficiency of Photosystem II (F_v/F_m) were used to assess the initial overall health of each coral sample following fragmentation, and prior to closed-system respirometry. Corals were acclimated under dark conditions (<5 μmol photons m^{-2} s^{-1}) for 15 min, then a Diving-PAM fluorometer (Walz GmbH, Germany) with attached fibreoptic cable was used to make three replicate measurements of each coral fragment (as per Hughes et al., 2022) using the following instrument settings: measuring light and saturating intensity 8, saturating pulse width 0.8 s, signal damping 3, and signal gain 2–4. Following ~30 min of travel, a seawater change of the cooler box was made, replacing 90 % of the volume with fresh seawater from the sampling site, before being transported from the boat for respirometry assessment.

Briefly, fragments were acclimated for 60 min in individual glass chambers (400 mL), maintaining DO at > 90 % of air saturation using air-stones connected to an air pump (Marina 200 Aquarium Air Pump), prior to airtight sealing and full submersion in a water bath maintained at 29 ± 0.5 °C by a heating immersion circulator (EH, JULABO, Julabo USA, Inc.). Fragments were placed on mesh platforms inside the chambers, allowing free rotation of a 30 × 7 mm magnetic stirring bar beneath (~500 rpm; PTFE, ROWE Scientific Pty Ltd), as controlled by a multi-station stirring plate (iStir HP 10M, Neuation Technologies Pty Ltd). Each chamber was fitted with an optical O_2 sensor spot (OXSP5, PyroScience, Germany) for contactless readout via a fibreoptic O_2 probe (SPFIB-BARE, PyroScience, Germany) connected to a FireSting-O_2 (PyroScience, Germany). Oxygen in the chambers (pO_2, % air sat) was continuously monitored (every 60 s) as the concentration changed from 100 % air saturation to 0 % O_2, until incubations were terminated, and mean O_2 consumption rates for each fragment were calculated (VO_2, mg O_2 h^{-1}). All rates were normalised to incubation volume using seawater displacement calculations, and seawater controls to account for microbial respiration. All O_2 probes and sensor spots were calibrated by measurements in 100 % air-saturated seawater and a 0 % O_2 solution with Na_2SO_3 solution prior to use. For more details on the closed-system respirometry methodology, see Dilernia et al. (2024).

All HRCs generated were fit with a 2-parameter Michaelis-Menten function as per Dilernia et al. (2024) using the RStudio packages "drc" v. 3.0.1 (Ritz et al., 2015) and "ggplot2" (Wickham, 2016). Relevant oxyregulatory descriptive parameters were then extracted from the fitted functions, including (i) the total positive or "average" regulation, T_{pos} (relative units), and (ii) the minimum/maximum pO_2 level at which oxyregulatory capacity is achieved, P_{cmin}/P_{cmax} (units in % air sat). Here, P_{cmax} also describes a hypoxic threshold, where O_2 regulation capacity can no longer increase past this point (Dilernia et al., 2024; Hughes et al., 2022). Since data did not pass parametric assumptions and subsequent data transformations failed, significant differences across site (WIML and LIRF) between the extracted parameters from each HRC fit were analysed via an Aligned Ranks Transform (ART) ANOVA with *post-hoc* interaction pairwise comparisons with Tukey's *p*-value adjustment method using RStudio installed packages "ARTool" (Kay et al., 2021; Wobbrock et al., 2011), "multcomp" (Hothorn et al., 2025), and "ggplot2" (Kassambara, 2023b; Wickham, 2016). We confirmed ART ANOVA assumptions by performing a Residual Alignment Check with QQ plots.

2.5. Gene expression analysis

Flash frozen coral samples (n = 4–5 fragments per treatment) were collected following CBASS experiments at 30, 33 and 36 °C, as per (Roper et al., 2025). For the current study, only samples in the 30 °C treatment were assessed, as the influence of thermal stress was not the intended focus of the work. Samples underwent total RNA extraction following the QIAGEN RNeasy mini kit protocol (QIAGEN, Germany). Prior to RNA extraction, coral tissue was removed from the holobiont samples via airbrushing, followed by tissue sample homogenisation and centrifugation steps. RNA quality was controlled via spectrophotometry (NanoDrop, 2000; ThermoFisher Scientific, Massachusetts, USA). Extracted RNA samples were sent to the Australian Genome Research Facility (AGRF, Melbourne, Aust.) for whole transcriptome sequencing, returning 2 x 150 bp paired-end mRNA libraries (of which, only specific GOIs related to the hypoxic response pathway from the 30 °C treatment were of interest for this particular study). The Illumina NovaSeq X 10B flow cell (300 cycles, with five additional lanes) was utilised for RNA sequencing. Full RNA extraction and sequencing details are given elsewhere (Roper et al., 2025).

Following quality control and trimming steps (FastQC v0.12.1 and Trimmomatic v0.39), demultiplexed reads were mapped to the reference genomic gene set (n = 33,730 predicted protein-coding genes) of Hawaiian *Pocillopora acuta* (Stephens et al., 2022). Read counts were quantified using the function 'quantMode GeneCounts' in STAR (v2.7.11b). HTSeq (v0.12.3) was used to estimate abundances of gene transcripts to generate count data (Anders et al., 2015). For the 30 °C treatment, normalised FPKMs (i.e., fragments per kilobase per million mapped reads) were estimated from: 1) HTSeq counts, and 2) fragment length calculated from 'CollectInsertSizeMetricsmodule' in Picard (v 3.1.1) (Broad Institute, 2019), using the R package countToFPKM (Alhendi, 2019). Functional gene annotation was inferred using the EggNOG v5.0 ortholog database by EMBL (Huerta-Cepas et al., 2019) annotation of the reference genome (Roper et al., 2025). Highly conserved metazoan genes associated with the hypoxia stress response in corals (Alderdice et al., 2021, 2022a, 2022b, 2022c) were selected based on their EggNOG description or gene name depending on availability, and their corresponding FPKM expression was plotted using the R package "ggplot2" (Wickham, 2016) to assess expression patterns across groups (M-R, WM, R-R, WR). FPKM expression estimates were summed for genes that shared the same functional annotation (e.g. *PCK1*) *sensu* Alderdice et al. (2021, 2022a). However, in the case that not all genes with the same functional annotation were differentially expressed (e.g. *ODH*), only those which were differentially expressed

were presented (e.g. only one transcript of *ODH* was plotted; see Table S2, Fig. S2). Patterns of the differentially expressed genes (DEGs) of the GOIs were indicated in plots in accordance to the differential expression analysis using DESeq2 (p-value cut-off <0.05) (Love et al., 2014) performed by (Roper et al., 2025) (see results for GOI in Table S2). The R-script and a full gene expression matrix are available at https://github.com/RachelCAlderdice/FPKM_analysis-Nikki, and the RNASeq data (FastQC) can be found at: http://www.ncbi.nlm.nih.gov/bioproject/1189141.

3. Results

3.1. Abiotic characterisation

Temperature and O_2 profiles measured at Woody Island mangrove lagoon (WIML) and Low Isles reef flat (LIRF) during the time of sampling generally appeared to reflect changes in tidal height, rather than diel cycles (i.e., time of day), specifically in the mangroves (Fig. 2a). DO content (mg O_2 L^{-1}) in WIML from 22nd – Feb 24, 2023 spanned 1.77–10.08 mg O_2 L^{-1}, reaching <2 mg O_2 L^{-1} daily (Fig. 2) i.e., below the widely accepted hypoxic threshold (Hughes et al., 2020) 3 % more of the time than in the reef habitat (Fig. 2b). From 2017 to 2023, the mean recorded DO measured in WIML ranged from ~3.36 to 6.85 mg O_2 L^{-1} ± SE 0.05 (averaged from historical and current logging data; see Table S3 for full sampling index and deployment date range; (Camp et al., 2019; Haydon et al., 2021; Ros et al., 2021). In comparison, LIRF exhibited a greater daily range of DO (>11 mg L^{-1}) from 3.96 to 15.03 mg O_2 L^{-1} (Fig. 2a), significantly higher than WIML ($t_{15752.24} = -19.85$, $p < 0.01$; Table S3), accumulating to 80 % of time spent >6 mg O_2 L^{-1} (Fig. 2b). Although LIRF had a higher mean temperature (28.82 °C ± SE 0.01) compared to WIML (27.95 °C ± SE 0.02; $t_{72.78}$, $p < 0.01$; Table S3), ambient temperature was much more variable in the mangroves than reef, with almost a three-fold higher range (>7 °C), spanning 23.85–31.20 °C, compared to LIRF, with 100 % of time logged between 28 and 29 °C; Fig. 2b).

3.2. P:R incubations (experiment 1)

Overall rates of gross photosynthesis and respiration were similar between groups, with the exception of wild mangrove (WM) corals, which exhibited significantly higher respiration rates than all other groups ($F_{3, 20} = 8.15$, $p < 0.01$; Table S4). Consequently, WM corals exhibited the lowest gross photosynthesis-to-respiration ratio (P_G:R 3.67) significantly different to all other groups ($F_{3, 20} = 57.69$, $p < 0.01$; Fig. 3b; Table S4). Notably, the mangrove-reef (M-R) coral transplant group did not show the same enhanced respiration as the WM (0.16 ± SE 0.02 µmol cm^{-2} h^{-1}; Fig. 3a). All of the P:R ratios measured across WIML and LIRF remained above one (Fig. 3b).

3.3. Hypoxia response curves (HRCs) (experiment 2)

Maximum photochemical efficiency (F_v/F_m) of Photosystem II measured in *P. acuta* fragments – following fragmentation and prior to incubation for HRCs in order to assess the initial overall health of each coral sample – ranged from 0.63 (WM) to 0.69 (M-R), with a mean F_v/F_m of 0.65 across all groups (seeFig. S3 for all F_v/F_m measurements). Overall, total average positive regulation (T_{pos}, relative) was similar between the four treatment groups (Fig. 4b). Values were marginally highest in the wild mangrove (WM) corals (T_{pos} = 1.69 ± SE 0.33) compared to all other groups, and 1.3 times greater than for the wild reef (WR) corals specifically (T_{pos} = 1.30 ± SE 0.19; Fig. 4b), albeit non-significant likely due to the high standard error (Fig. 4b; Table S5). Notably, fragments of *P. acuta* from all four groups exhibited values for the hypoxic threshold for upregulation (P_{cmax}, % air sat) at relatively low pO_2 levels, i.e., all below 13 % air saturation (~1 mg O_2 L^{-1}), with significant differences across the groups ($F_{3,20} = 16.80$, $p < 0.01$; Fig. 4c; Table S5). Specifically, M-R coral transplants yielded a considerably lower P_{cmax} (2.50 % air saturation ± SE 0.56), as compared to both the

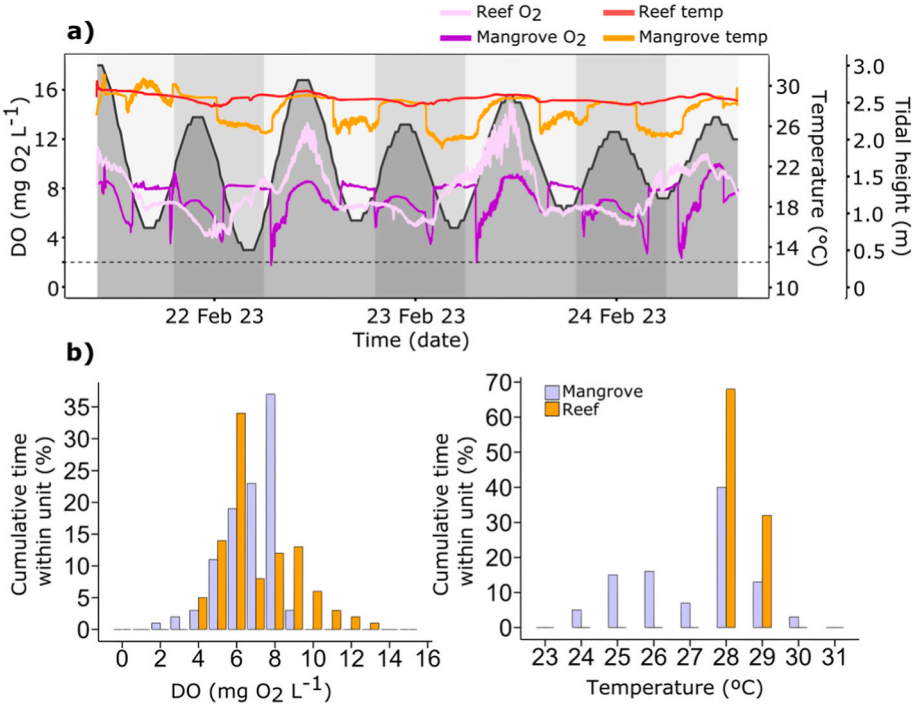

Fig. 2. a) Dissolved oxygen (DO) content (mg O_2 L^{-1}; left y-axis) and ambient water temperature (°C; inside right y-axis) measured at Woody Island mangrove lagoon (WIML) and Low Isles reef flat (LIRF), from loggers deployed during sampling dates of *Pocillopora acuta* colonies. Additionally, tidal height (m; dark shaded area with black outline) on the outside right y-axis has been coupled with daily light cycles, as represented by vertical shading over time on the x-axis (date). Dashed horizontal line represents hypoxia (i.e., 2 mg O_2 L^{-1}). **b)** Cumulative time of DO content and temperature measured within WIML and LIRF. Bars represent the cumulative time within unit (y-axes, %), where the measurements taken in each habitat (mangrove, reef) were within the specific DO and temperature (x-axes) levels.

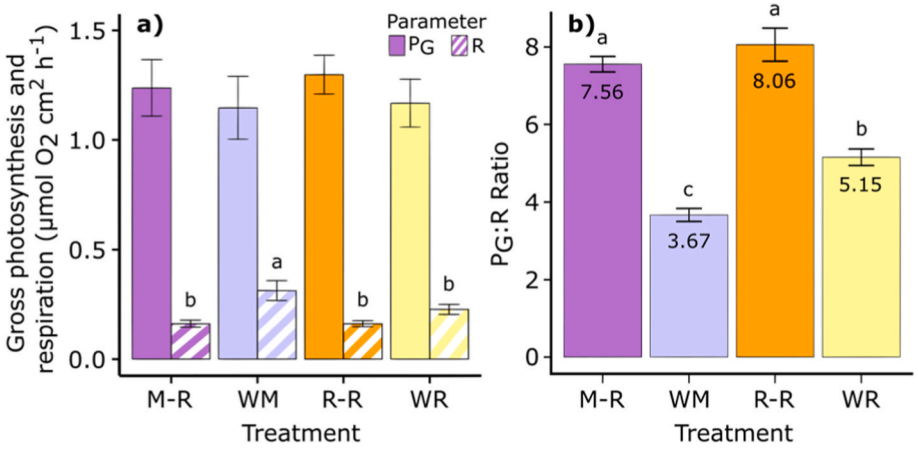

Fig. 3. a) Comparison of gross photosynthesis (P_G) and respiration (R) (µmol O_2 cm^{-2} h^{-1}) ± SE from P:R incubations of the four groups of *Pocillopora acuta*, including mangrove-reef (M–R), wild mangrove (WM), reef-reef (R–R), and wild reef (WR), from Woody Island mangrove lagoon (WIML) and Low Isles reef flat (LIRF). Solid colour barplots denote P_G, striped barplots denote R. **b)** Calculated ratios of $P_{G:}R$ (dimensionless) for each group. All error bars denote standard error (n = 6). Significant *post-hoc* differences between groups (Tukey HSD, where p-value <0.05) are indicated with a lowercase letter (e.g., "a"), where one group is significantly different in comparison to all other groups.

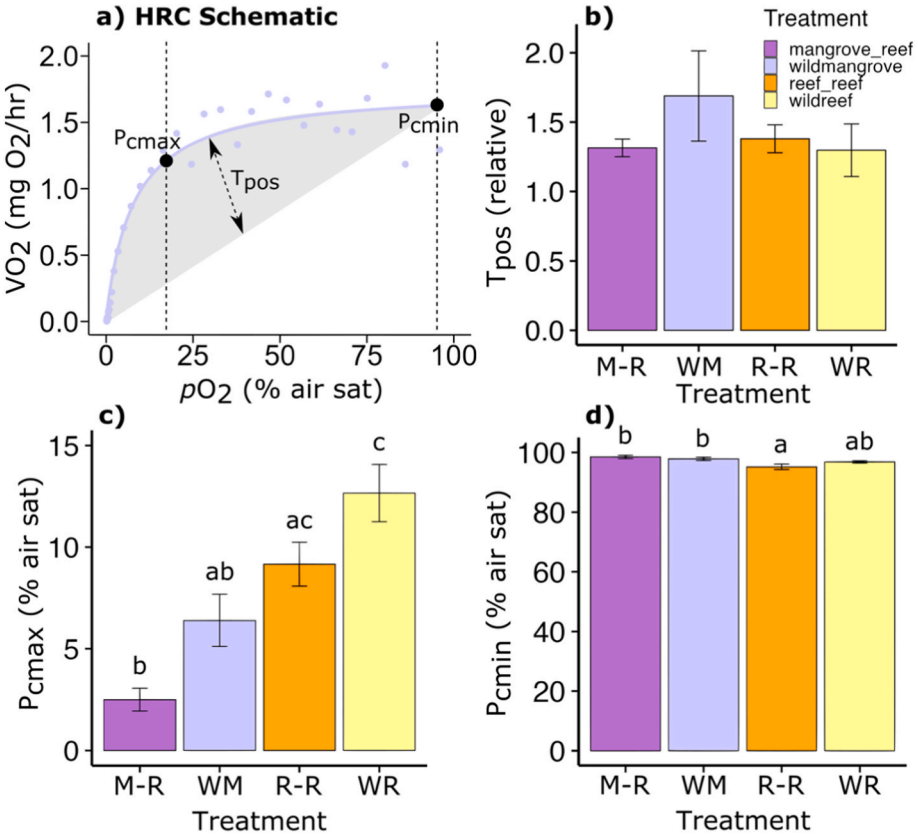

Fig. 4. a) Schematic diagram outlining points of extraction for hypoxia response curve (HRC) parameters (T_{pos}, P_{cmax}, P_{cmin}). **(b–d)** Comparison of the mean extracted parameters (T_{pos}, P_{cmax}, P_{cmin}) from four groups of *Pocillopora acuta* HRC datasets fit with a Michaelis-Menten function, including mangrove-reef (M–R), wild mangrove (WM), reef-reef (R–R), and wild reef (WR), from Woody Island mangrove lagoon and Low Isles reef flat. Error bars denote standard error (n = 6). Significant *post-hoc* differences between groups (Tukey's HSD, where p-value <0.05) are indicated with a lowercase letter (e.g., "a"), where significant differences are denoted by different letters.

R-R transplant (9.17 % air saturation ± SE 1.08; $t_{20} = -4.70$, $p < 0.01$) and WR corals (12.67 % air saturation ± SE 1.41; $t_{20} = -6.83$, $p < 0.01$) (Table S5). The WR control was also almost two-fold higher than the WM control ($t_{20} = -3.90$, $p < 0.01$), with the WM P_{cmax} value of 6.40 % air saturation ± SE 1.29 (~0.49 mg O_2 L^{-1}), which interestingly was similar to the R-R transplant P_{cmax} (Fig. 4c).

Minimum regulation capacity (P_{cmin}, % air sat) spanned pO_2 values of 95.17–98.50 % air saturation across the groups (Fig. 4d). The R-R transplant P_{cmin} value (95.17 % air saturation) was lower than both the M-R (P_{cmin} = 98.50 % air saturation; $t_{20} = 3.81$, $p = 0.01$) and WM (P_{cmin} = 97.83 % air saturation; $t_{20} = -2.88$, $p = 0.04$), exhibiting the lowest threshold for minimum regulation capacity (Fig. 4d; Table S5).

To further compare metabolic functioning and physiology with oxy-regulatory capacity under low-pO_2 conditions, we next examined for any correspondence between the gross photosynthesis-to-respiration ratio (P_G:R) and the HRC extracted oxyregulatory parameters (T_{pos}, P_{cmax}, P_{cmin}), across each of the four groups (Fig. S4). A moderate negative correlation was evident between T_{pos} and the P_G:R ratio with a coefficient of determination (R^2) of 0.45, and Pearson's correlation coefficient (R) of −0.67. In general, a higher P_G:R ratio correlated to a lower T_{pos} (Fig. S4a) – for example, WM corals exhibited the lowest P_G:R ratio (3.67) and highest T_{pos} (1.69). That said, no statistically significant differences were evident between the means of the groups for the linear regression ($F_{1,\ 2} = 1.68$, $p = 0.32$).

3.4. Gene expression analysis

Expression patterns for genes previously associated with coral hypoxic stress response were examined across the four transplant groups to identify potential mechanisms governing any differences in hypoxic responses between reef and mangrove corals (pre- and post-transplantation). Gene expression based on FPKM of the hypoxia-inducible factor alpha subunit (*HIF1A*) was significantly highest in the wild reef (WR) corals (Fig. 5a) compared to corals transplanted onto the reef (R-R and M-R; WR vs R-R Log_2 fold change (FC_{log2}) = 0.57, $p < 0.05$; WR vs M-R $FC_{log2} = 0.59$, $p < 0.05$), and yet similar to the wild mangrove controls (WM; Table S2). The increase of HIF1A in WR corresponded to significantly higher expression of HIF-targets Lactate Dehydrogenase (*LDHB*) (WR FC_{log2} vs M-R = 1.67; R-R = 1.00; WM = 1.22), Pyruvate Dehydrogenase Kinase (*PDK2*) (WR FC_{log2} vs M-R = 0.92; R-R = 1.00; WM = 0.80), and Phosphoenolpyruvate Carboxykinase (*PCK1*) (WR FC_{log2} vs M-R = 1.18; R-R = 1.34; WM = 1.55) in this group (Fig. 5d–f, all $p < 0.05$; see also Table S2), suggesting induction of the HIF hypoxia response pathway in WR. However, Prolyl Hydroxylase Domain 2 (*PHD2/EGLN1*) – a HIF transcriptional inhibitor known to suppress the *HIF1A* gene under low-pO_2 conditions (Kaelin and Ratcliffe, 2008), in corals (Alderdice et al., 2022a) – was overexpressed in the wild mangrove (WM), and significantly higher than all other groups ($p < 0.05$; Fig. 5b–Table S2). Similarly, WM was also characterised by upregulation of the non-HIF targeted GOI Octopine Dehydrogenase (*ODH*; Fig. 5c) – an alternative means of anaerobic respiration found in invertebrates (Harcet et al., 2013; Murphy and Richmond, 2016) – and differentially expressed from M-R (FC_{log2} = - 1.15, $p < 0.05$). Additionally, expression of ODH was also found to differ between M-R and WR corals (FC_{log2} = - 0.88, $p < 0.05$; Table S2). Other GOIs, including Heat shock protein 90 (*HSP90B1*) and Heme oxygenase (*HMOX1*) – related to formation of the 'active HIF complex', and another HIF-target, respectively (Alderdice et al., 2021, 2022a) – were highest in the mangrove corals (M-R and WM), but were not differentially expressed (see Fig. S2).

To further compare the expression of key hypoxia response genes with coral oxyregulatory capacity under low-pO_2 conditions, we examined for any correlation between the targeted GOI's (e.g., *HIF1A* etc) and the HRC extracted oxyregulatory parameters (T_{pos}, P_{cmax}, P_{cmin}), across each of the four coral groups (Fig. S5). In all relationships between gene expression counts (FPKMs) and P_{cmax} value (% air sat) – except for *PHD2/EGLN1*, which more closely followed the pattern of T_{pos} (relative) – there was a positive correlation where a higher gene expression generally correlated to a higher P_{cmax} value (i.e., higher threshold for O_2 upregulation). The strongest correlation was found between *LDBH* and P_{cmax} – where the WR group had the highest *LDBH* expression and highest P_{cmax} (while the M-R had the lowest of both) – with a Pearson's correlation coefficient (R) of 0.92 ($R^2 = 0.85$), albeit not significant ($F_{1,\ 2} = 11.12$, $p = 0.08$; Fig. S5). Opposingly for T_{pos}, majority of

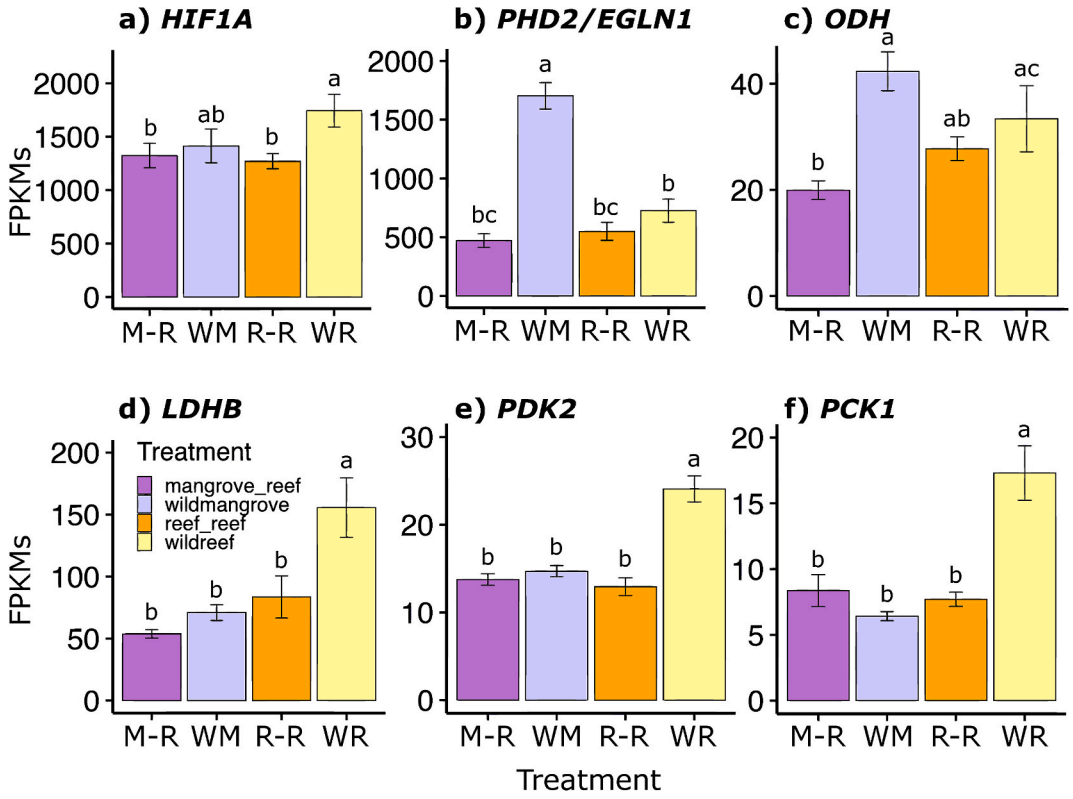

Fig. 5. (a–f) Expression patterns of key hypoxia stress response genes, based on fragments per kilobase of transcript per million mapped reads (FPKM) for genes of interest; a) Hypoxia-Inducible Factor alpha subunit (*HIF1A*), b) Prolyl Hydroxylase domain 2 (*PHD2/EGLN1*), c) Octopine Dehydrogenase (*ODH*), and HIF targets including d) Lactate Dehydrogenase (*LDHB*), e) Pyruvate Dehydrogenase Kinase (*PDK2*), and f) Phosphoenolpyruvate Carboxykinase (*PCK1*). Error bars denote standard error with $n = 4$ to 5). Groups include mangrove-reef (M–R), wild mangrove (WM), reef-reef (R–R), and wild reef (WR). Significant differential expression (p-value cut-off <0.05) are indicated with lowercase letters (e.g., "a"), where significant differences are denoted by different letters.

relationships with GOI's were negatively correlated, where an increase in the gene expression led to a decrease in T_{pos} – again, except for *PHD2/EGLN1* and *ODH*, which both showed strong positive correlations (R = 0.94 and 0.77, respectively; Fig. S5).

4. Discussion

Assessing the hypoxia tolerance of corals using long-term transplantation between a relatively extreme reef-neighbouring habitat and comparatively more stable reef environment (e.g., Haydon et al., 2021) provides a means to advance insight into capacity for corals enduring low-pO_2 conditions. Our results demonstrate that *P. acuta* from the mangrove lagoons and reef flat employ a relatively similar average oxyregulation capacity while surviving in these contrasting environments, and yet the mangrove corals exert a maximum capacity for oxyregulation at a significantly lower hypoxic threshold that is retained after being translocated to the neighbouring reef for a 1-year period. Retention of a lower hypoxic threshold for O_2 upregulation (where maintenance of a constant VO_2 ceases, and regulation capacity can no longer increase past this point), may speak to a conserved property attributed to their frequent exposure to periodic hypoxia (O_2 < 2 mg L^{-1}; see Hughes et al., 2020) in this extreme mangrove habitat (Scucchia et al., 2023). Moreover, these oxyregulation trends coincide with the differential expression of hypoxia response GOIs consistent with "pre--conditioning" for low-O_2 thresholds, where thermal pre-conditioning in *P. acuta* has also been shown to increase gene expression to alleviate oxidative damage (Majerová and Drury, 2022). Our study shows that the inherent exposure to hypoxic conditions and temperature fluctuations in the extreme mangrove lagoon, has indeed selected for more a resistant *P. acuta* population, able to persist under variable and low-pO_2 seawater conditions, even after being moved to a new environment.

4.1. Inherent environmental characteristics of extreme environments

In accordance with prior studies conducted at Woody Island mangrove lagoon (WIML), we documented extreme low-pO_2 and highly variable seawater temperatures. DO concentrations at WIML dropped below 1.77 mg O_2 L^{-1} on a daily basis (Fig. 2), i.e., below the hypoxic threshold widely referred to in the literature (<2 mg L^{-1}; e.g., Diaz and Rosenberg, 1995; Rabalais et al., 2001; Vaquer-Sunyer and Duarte, 2008; Steckbauer et al., 2011; Altieri et al., 2017; Hughes et al., 2020), subjecting native mangrove *P. acuta* to frequent low-pO_2 exposure. Historically, the daily DO in WIML has averaged just 3.36 mg O_2 L^{-1} ± SE 0.05 (Camp et al., 2019; Haydon et al., 2021), as compared to ~6.50 mg L^{-1} on Low Isles reef flat (LIRF) (Haydon et al., 2021), and mangrove seawater temperatures reached >29 °C on a daily basis (Table S3). Prior studies have shown that exposure to extreme and/or highly variable environmental conditions can pre-condition corals to low pH and variable temperatures (e.g., Camp et al., 2016). Here we reveal that frequent low-pO_2 exposure and temperature fluctuations in this extreme environment appears to have influenced the mangrove corals retention of a low maximum regulation capacity (P_{cmax}), i.e., the ability to continue to oxyregulate at a significantly lower hypoxic threshold, where inherent extreme environmental conditions have over time pre-conditioned mangrove corals to higher temperatures (see Roper et al., 2025) and low-pO_2 availability.

4.2. Retention of low coral P_{cmax} following transplantation

In terms of broad range oxyregulatory capacity, our data showed similar average T_{pos} values across all corals (including transplants). Although the wild mangrove (WM) fragments did have a ~30 % higher T_{pos} in comparison to corals native to the adjacent reef (wild reef; WR), this was not statistically significant, and the mangrove-reef (M-R) transplants more closely followed the reef corals (Fig. 4b). Additional longer-term monitoring (i.e., > 1-year) may further elucidate any conserved properties of the transplanted *P. acuta* population over time. Nonetheless, average oxyregulatory capacity ranged from 1.30 to 1.69 (T_{pos}, relative) for all corals from both the mangrove and reef (Fig. 4b), i.e., higher than values obtained for diverse species of *Acropora* (from Opal Reef in Feb 2022, ~40 km NE of Low Isles on the GBR), which exhibited a more variable range of hypoxic tolerance, from 0.60 to 1.03 (T_{pos}) (Dilernia et al., 2024). Furthermore, *P. acuta* has previously demonstrated a particularly high T_{pos} (>2.00) (Hughes et al., 2022), with fragments of this particular species collected and analysed from Opal Reef (GBR, Aug 2018).

The WM corals also appeared to induce a non-HIF target pathway as an alternative means of anaerobic respiration by stimulating *ODH* expression (Alderdice et al., 2022a; Harcet et al., 2013) and down-regulating *LDH* (Fig. 5c and d). Indeed, *ODH* has been a favored pathway across marine invertebrates in helping to support corals under prolonged hypoxia or hypometabolism (Alderdice et al., 2022a; Murphy and Richmond, 2016). In addition, an overexpression of *PHD2/EGLN1* (WM; Fig. 5b) can imply vulnerability to low-pO_2 conditions (Alderdice et al., 2022b), however the specific induction of this GOI due to prolonged hypoxia exposure can alternatively indicate a certain level of hypoxia tolerance, as *PHD2/EGLN1* overexpression activates negative feedback in the HIF-hypoxia response pathway using available intra-cellular O_2 to prevent cell death by *HIF1A* proteolysis (Alderdice et al., 2022b). Expression of these GOI's (*ODH* and *PHD2/EGLN1*) closely followed the trends of the T_{pos} values (with strong positive correlations; Fig. S5), where corals from the mangroves behaved more similarly to reef corals following transplantation.

These findings are consistent with the higher rates of respiration measured in the WM corals (0.31 ± SE 0.05 μmol cm^{-2} h^{-1}; Fig. 3), and mirror trends in WIML corals previously analysed (Camp et al., 2016, 2019). Enhanced respiration rates followed a reduction in net photosynthesis (Camp et al., 2017, 2019; Ros et al., 2021), suggesting increased heterotrophy to facilitate coral survival in the extreme ecosystem (Camp et al., 2019; Simancas-Giraldo et al., 2021). Although the coral populations of the mangrove lagoons generally carry greater densities of Symbiodiniaceae – associating with the thermally-tolerant genus *Durusdinium* (Camp et al., 2019; Ros et al., 2021) – the mangrove-reef (M-R) transplant corals did not show the same trend in photosynthesis-to-respiration as the WM coral, rather corresponding more closely with the metabolic signatures of the reef-reef (R-R) transplants (Fig. 3). However, all P_G:R ratios calculated here were above the "compensation threshold" (P:R > 1.00; see Fig. 3b) (Simancas-Giraldo et al., 2021).

All measured P_{cmax} values were <1 mg O_2 L^{-1}, indicating a low threshold for hypoxic upregulation in corals across both the WIML and LIRF environments. Most notably, the transplanted mangrove corals in our current study (M-R) returned the lowest P_{cmax} value on average (<3 % air sat; Fig. 4c). Generally, a lower P_{cmax} (or "P_{crit}"; i.e., the critical O_2 tension (Cobbs and Alexander, 2018; Seibel et al., 2021)), enables organisms to maintain oxyregulation for longer under decreasing O_2 conditions, lowering the threshold for hypoxic upregulation which is considered most advantageous for surviving low-pO_2 periods (Mandic et al., 2020; Pontes et al., 2023). Specific retention of a low P_{cmax} in the M-R coral transplant aligns with retention of increased thermal tolerance properties (Roper et al., 2025), where corals retained an average thermal tolerance up to ~37.45 °C (± SE 0.30) over a year after being transplanted from mangrove-to-reef (Roper et al., 2025). Indeed, local adaptation and/or acclimation can occur following frequent exposure of corals to stressful conditions (Palumbi et al., 2014; Scucchia et al., 2023), including increasingly high temperatures (e.g., Silbiger et al., 2019; Banc-Prandi et al., 2022; Haydon et al., 2023), low-pH (e.g., Golbuu et al., 2016; Camp et al., 2017), and low, albeit not hypoxic, O_2 levels (3 mg L^{-1}) (Maggioni et al., 2021). The retention of a favourable low P_{cmax} (in addition to thermotolerance (Roper et al., 2025) highlights the capacity of the mangrove *P. acuta* corals to survive in extreme O_2 coral habitats following transplantation (Schoepf et al., 2023; Scucchia

et al., 2023).

Surprisingly, expression of the hypoxia-inducible factor (*HIF1A*) was similar across the treatment groups, with only the WR corals showing greater upregulation in comparison to both transplant groups (M-R, R-R; Fig. 5a). This, coupled with a significantly higher P_{cmax} than all corals originating from the mangroves (Fig. 4c), may suggest that hypoxic stress triggered an upregulation of the HIF-hypoxia response pathway in corals native to the reef (WR), activating an increase in the supply of O_2 to the corals tissues for survival (Röning et al., 2022). Although transient upregulation of *HIF1A* under hypoxic conditions is generally beneficial for short-term stress by reducing energy-consumption, prolonged upregulation could have negative long-term effects on coral metabolism causing energy imbalance and inefficiency, e.g., under prolonged glycolysis (Murphy and Richmond, 2016). Activation of *HIF1A* can also increase production of reactive oxygen species (ROS) and oxidative stress (Bae et al., 2024; Qutub and Popel, 2008). Heat shock protein 90 (*HSP90B1*) and HIF-target Heme oxygenase (*HMOX1*) were other GOIs found to have increased expression in the mangrove corals (Fig. S2). However, they did not follow patterns similar to the other HIF genes, despite *HSP90* has been proposed to be a cofactor of *HIF1A*, regulating HIF target genes (Alderdice et al., 2021). The genetic findings in this study most interestingly suggest that there's quite a lot of similarity between the transplanted reef and mangrove corals, but that the wild reef and wild mangrove corals behave differently. Given the observed physiological and gene expression differences here, further exploration of the distinct genetic patterns exhibited across these different environments would provide deeper insight into the adaptive and/or acclimatory properties of the *P. acuta* coral populations.

4.3. Conclusion

Extreme reef-neighbouring mangrove systems are harbouring corals exhibiting an increased capacity to retain a lower threshold for hypoxic upregulation, due to routine exposure to low-pO_2 conditions conventionally considered hypoxic. These attributes could be considered advantageous against the continued loss of dissolved O_2 concentrations in the global oceans (Altieri et al., 2021; Hughes et al., 2020; Levin, 2018). Following a 1-year long transplantation of *P. acuta* between Low Isles reef flat and Woody Island mangrove lagoon to analyse coral hypoxia tolerance, we have shown: (1) significant differences in the hypoxic response of this tropical coral, specifically (2) higher oxyregulation capacity of native mangrove corals, (3) with transplanted mangrove-to-reef corals exerting a maximum regulation capacity at a significantly lower hypoxic threshold that is retained after a 1-year translocation period, and (4) diverse photosynthesis:respiration trade-offs and patterns of non-HIF-hypoxia response pathway upregulation facilitating coral survival in the extreme ecosystem, in contrast to habitats where dissolved O_2 content remains comparatively high. We acknowledge that the gene expression patterns of the HIF-mediated hypoxia response systems observed here cannot entirely explain the specific cellular mechanisms underlying the physiological acclimatisation of these extreme corals without accompanying proteomics. However, based solely on the physiological data and gene expression patterns observed here, we conclude that these results collectively highlight the potential tolerance of mangrove *P. acuta* as an oxyregulator to survive low-pO_2 conditions across habitats, indicating that hypoxic tolerance may be a long-term conserved response to surviving in an extreme coral habitat, which appears advantageous both now and under future projected climate change conditions.

CRediT authorship contribution statement

Nicole J. Dilernia: Writing – review & editing, Writing – original draft, Visualization, Validation, Software, Resources, Methodology, Investigation, Funding acquisition, Formal analysis, Data curation, Conceptualization. **David J. Suggett:** Writing – review & editing, Supervision, Methodology, Conceptualization. **Christine D. Roper:** Writing – review & editing, Software, Formal analysis, Data curation. **Rachel Alderdice:** Writing – review & editing, Software, Formal analysis, Data curation. **Christian R. Voolstra:** Writing – review & editing. **Michael Kühl:** Writing – review & editing, Resources. **Emma F. Camp:** Writing – review & editing, Supervision, Resources, Project administration, Methodology, Funding acquisition, Conceptualization.

Funding

This research was supported by anAustralian Government Research Training Program Scholarship (N.J.D.), and an Australian Research Council Discovery Project (DP230100210) (awarded to: D.J.S., E.F.C., and M.K.). M.K. also acknowledges additional support from the Gordon and Betty Moore Foundation (grant no. GBMF9206; https://doi.org/10.37807/GBMF9206).

Declaration of competing interest

The authors declare the following financial interests/personal relationships which may be considered as potential competing interests: Nicole J. Dilernia reports financial support was provided by Australian Government Research Training Program. Emma F. Camp, David J. Suggett, Michael Kuhl reports financial support was provided by Australian Research Council Discovery Project. Michael Kuhl reports a relationship with Gordon and Betty Moore Foundation that includes: funding grants. If there are other authors, they declare that they have no known competing financial interests or personal relationships that could have appeared to influence the work reported in this paper.

Acknowledgements

We wish to acknowledge and pay our respects to the Traditional Owners and Custodians of the land and sea country on which this field work was conducted – the Yirrganydji people, of the Cairns to Port Douglas region, QLD. The authors wish to express thanks to the owners and staff of Wavelength Reef Cruises for their invaluable knowledge of the region, and assistance in providing reef access. As well as the Great Barrier Reef Marine Park Authority for their continued support and issuance of Permit No. G18/40023.1, and Fisheries Permit No. 260065. N.J.D. would also like to personally thank Future Reefs Team members Hadley England, Jaz Carroll and Chiara Duijser for their assistance during field work and sample collection in Feb 2023.

Appendix A. Supplementary data

Supplementary data to this article can be found online at https://doi.org/10.1016/j.envres.2025.122740.

Data availability

I have shared the link to my data/code in a Data Availability statement in the manuscript

References

Alderdice, R., Hume, B.C.C., Kühl, M., Pernice, M., Suggett, D.J., Voolstra, C.R., 2022a. Disparate inventories of hypoxia gene sets across corals align with inferred environmental resilience. Front. Mar. Sci. 9, 834332. https://doi.org/10.3389/FMARS.2022.834332/BIBTEX.

Alderdice, R., Perna, G., Cárdenas, A., Hume, B.C.C., Wolf, M., Kühl, M., Pernice, M., Suggett, D.J., Voolstra, C.R., 2022b. Deoxygenation lowers the thermal threshold of coral bleaching. Sci. Rep. 12 (1 12), 1–14. https://doi.org/10.1038/s41598-022-22604-3, 2022.

Alderdice, R., Pernice, M., Cárdenas, A., Hughes, D.J., Harrison, P.L., Boulotte, N., Chartrand, K., Kühl, M., Suggett, D.J., Voolstra, C.R., 2022c. Hypoxia as a physiological cue and pathological stress for coral larvae. Mol. Ecol. 31, 571–587. https://doi.org/10.1111/mec.16259.

Alderdice, R., Suggett, D.J., Cárdenas, A., Hughes, D.J., Kühl, M., Pernice, M., Voolstra, C.R., 2021. Divergent expression of hypoxia response systems under deoxygenation in reef-forming corals aligns with bleaching susceptibility. Glob. Change Biol. 27. https://doi.org/10.1111/gcb.15436.

Alhendi, A., 2019. countToFPKM: convert counts to fragments per kilobase of transcript per million (FPKM). R package version 1.0.0. https://github.com/AAlhendi1707/countToFPKM.

Altieri, A.H., Harrison, S.B., Seemann, J., Collin, R., Diaz, R.J., Knowlton, N., 2017. Tropical dead zones and mass mortalities on coral reefs. Proceedings of the National Academy of Sciences of the United States of America 114, 3660–3665. https://doi.org/10.1073/pnas.1621517114.

Altieri, A.H., Johnson, M.D., Swaminathan, S.D., Nelson, H.R., Gedan, K.B., 2021. Resilience of tropical ecosystems to ocean deoxygenation. Trends Ecol. Evol. 36, 227–238. https://doi.org/10.1016/j.tree.2020.11.003.

Alva García, J.V., Klein, S.G., Alamoudi, T., Arossa, S., Parry, A.J., Steckbauer, A., Duarte, C.M., 2022. Thresholds of hypoxia of two Red Sea coral species (porites sp. and Galaxea fascicularis). Front. Mar. Sci. 9. https://doi.org/10.3389/fmars.2022.945293.

Anders, S., Pyl, P.T., Huber, W., 2015. HTSeq—a python framework to work with high-throughput sequencing data. Bioinformatics 31, 166–169. https://doi.org/10.1093/bioinformatics/btu638.

Bae, T., Hallis, S.P., Kwak, M.-K., 2024. Hypoxia, oxidative stress, and the interplay of HIFs and NRF2 signaling in cancer. Exp. Mol. Med. 56, 501–514. https://doi.org/10.1038/s12276-024-01180-8.

Banc-Prandi, G., Evensen, N.R., Barshis, D.J., Perna, G., Omar, Y.M., Fine, M., 2022. Assessment of temperature optimum signatures of corals at both latitudinal extremes of the Red Sea. Conservation Physiology 10. https://doi.org/10.1093/conphys/coac002.

Bartels, N., Dilernia, N.J., Howlett, L., Camp, E.F., 2023. Stress event for "super corals" in great Barrier reef mangrove lagoon. Mar. Biodivers. 53, 64. https://doi.org/10.1007/s12526-023-01374-9.

Breitburg, D., Levin, L.A., Oschlies, A., Grégoire, M., Chavez, F.P., Conley, D.J., Garçon, V., Gilbert, D., Gutiérrez, D., Isensee, K., Jacinto, G.S., Limburg, K.E., Montes, I., Naqvi, S.W.A., Pitcher, G.C., Rabalais, N.N., Roman, M.R., Rose, K.A., Seibel, B.A., Telszewski, M., Yasuhara, M., Zhang, J., 2018. Declining oxygen in the global ocean and coastal waters. Science 359. https://doi.org/10.1126/science.aam7240.

Broad Institute, 2019. Picard Tool Kit. GitHub Repository. https://broadinstitute.github.io/picard/.

Camp, E.F., Clases, D., Bishop, D., Dowd, A., Goyen, S., Gonzalez De Vega, R., Strudwick, P., Suggett, D.J., 2025. Coral elementomes diverge for colonies persisting in vegetative Lagoons versus reef environments. Sci. Total Environ. 979, 179455. https://doi.org/10.1016/j.scitotenv.2025.179455.

Camp, E.F., Edmondson, J., Doheny, A., Rumney, J., Grima, A.J., Huete, A., Suggett, D.J., 2019. Mangrove lagoons of the Great Barrier reef support coral populations persisting under extreme environmental conditions. Mar. Ecol. Prog. Ser. 625, 1–14. https://doi.org/10.3354/meps13073.

Camp, E.F., Nitschke, M.R., Rodolfo-Metalpa, R., Houlbreque, F., Gardner, S.G., Smith, D.J., Zampighi, M., Suggett, D.J., 2017. Reef-building corals thrive within hot-acidified and deoxygenated waters. Sci. Rep. 7. https://doi.org/10.1038/s41598-017-02383-y.

Camp, E.F., Schoepf, V., Mumby, P.J., Hardtke, L.A., Rodolfo-Metalpa, R., Smith, D.J., Suggett, D.J., 2018. The future of coral reefs subject to rapid climate change: lessons from natural extreme environments. Front. Mar. Sci. 5. https://doi.org/10.3389/fmars.2018.00004.

Camp, E.F., Suggett, D.J., Gendron, G., Jompa, J., Manfrino, C., Smith, D.J., 2016. Mangrove and seagrass beds provide different biogeochemical services for corals threatened by climate change. Front. Mar. Sci. 3. https://doi.org/10.3389/fmars.2016.00052.

Cobbs, G.A., Alexander, J.E., 2018. Assessment of oxygen consumption in response to progressive hypoxia. PLoS One 13. https://doi.org/10.1371/journal.pone.0208836.

De Mutsert, K., Steenbeek, J., Lewis, K., Buszowski, J., Cowan, J., Christensen, V., 2015. Exploring effects of hypoxia on fish and fisheries in the northern Gulf of Mexico using a dynamic spatially explicit ecosystem model. Ecol. Model. 331. https://doi.org/10.1016/j.ecolmodel.2015.10.013.

Deleja, M., Paula, J.R., Repolho, T., Franzitta, M., Baptista, M., Lopes, V., Simão, S., Fonseca, V.F., Duarte, B., Rosa, R., 2022. Effects of hypoxia on coral photobiology and oxidative stress. Biology 11, 1068. https://doi.org/10.3390/biology11071068.

Diaz, R., Rosenberg, R., 1995. Marine benthic hypoxia: a review of its ecological effects and the behavioural response of benthic macrofauna. Oceanography and marine biology. An annual review [Oceanogr. Mar. Biol. Annu. Rev. 33, 245–303.

Dilernia, N.J., Woodcock, S., Camp, E.F., Hughes, D.J., Kühl, M., Suggett, D.J., 2024. Intra-colony spatial variance of oxyregulation and hypoxic thresholds for key acropora coral species. Ecol. Evol. 14, e11100. https://doi.org/10.1002/ece3.11100.

Duijser, C.M., Nitschke, M.R., Rassmussen, S., Camp, E.F., 2025. Pocillopora host–symbiont interactions along an extreme environmental gradient. Coral Reefs. https://doi.org/10.1007/s00338-025-02672-3 (in press).

Evensen, N.R., Parker, K.E., Oliver, T.A., Palumbi, S.R., Logan, C.A., Ryan, J.S., Klepac, C.N., Perna, G., Warner, M.E., Voolstra, C.R., Barshis, D.J., 2023. The coral bleaching automated Stress system (CBASS): a low-cost, portable system for standardized empirical assessments of coral thermal limits. Limnol Oceanogr. Methods 21, 421–434. https://doi.org/10.1002/lom3.10555.

Golbuu, Y., Gouezo, M., Kurihara, H., Rehm, L., Wolanski, E., 2016. Long-term isolation and local adaptation in Palau's nikko Bay help corals thrive in acidic waters. Coral Reefs 35, 909–918. https://doi.org/10.1007/s00338-016-1457-5.

Haas, A.F., Smith, J.E., Thompson, M., Deheyn, D.D., 2014. Effects of reduced dissolved oxygen concentrations on physiology and fluorescence of hermatypic corals and benthic algae. PeerJ. https://doi.org/10.7717/peerj.235, 2014.

Harcet, M., Perina, D., Pleše, B., 2013. Opine dehydrogenases in marine invertebrates. Biochem. Genet. 51, 666–676. https://doi.org/10.1007/s10528-013-9596-7.

Haydon, T.D., Matthews, J.L., Seymour, J.R., Raina, J.-B., Seymour, J.E., Chartrand, K., Camp, E.F., Suggett, D.J., 2023. Metabolomic signatures of corals thriving across extreme reef habitats reveal strategies of heat stress tolerance. Proc. Biol. Sci. 290. https://doi.org/10.1098/RSPB.2022.1877.

Haydon, T.D., Seymour, J.R., Raina, J.B., Edmondson, J., Siboni, N., Matthews, J.L., Camp, E.F., Suggett, D.J., 2021. Rapid shifts in bacterial communities and homogeneity of symbiodiniaceae in colonies of Pocillopora acuta transplanted between reef and mangrove environments. Front. Microbiol. 12. https://doi.org/10.3389/FMICB.2021.756091/FULL.

Hoegh-Guldberg, O., 2011. Coral reef ecosystems and anthropogenic climate change. Reg. Environ. Change 11, 215–227. https://doi.org/10.1007/s10113-010-0189-2.

Hothorn, T., Bretz, F., Westfall, P., Heiberger, R.M., Schuetzenmeister, A., Scheibe, S., 2025. Multcomp: simultaneous inference in general parametric models, Version 1.4-28. https://cran.r-project.org/web/packages/multcomp/index.html.

Huerta-Cepas, J., Szklarczyk, D., Heller, D., Hernández-Plaza, A., Forslund, S.K., Cook, H., Mende, D.R., Letunic, I., Rattei, T., Jensen, L.J., von Mering, C., Bork, P., 2019. eggNOG 5.0: a hierarchical, functionally and phylogenetically annotated orthology resource based on 5090 organisms and 2502 viruses. Nucleic Acids Res. 47, D309–D314. https://doi.org/10.1093/nar/gky1085.

Hughes, D.J., Alderdice, R., Cooney, C., Kühl, M., Pernice, M., Voolstra, C.R., Suggett, D.J., 2020. Coral reef survival under accelerating ocean deoxygenation. Nat. Clim. Change 10, 296–307. https://doi.org/10.1038/s41558-020-0737-9.

Hughes, D.J., Alexander, J., Cobbs, G., Kühl, M., Cooney, C., Pernice, M., Varkey, D., Voolstra, C.R., Suggett, D.J., 2022. Widespread oxyregulation in tropical corals under hypoxia. Mar. Pollut. Bull. 179, 113722. https://doi.org/10.1016/J.MARPOLBUL.2022.113722.

IPCC, 2023. Summary for policymakers. In: Lee, H., Romero, J. (Eds.), Climate Change 2023: Synthesis Report. Contribution of Working Groups I, II and III to the Sixth Assessment Report of the Intergovernmental Panel on Climate Change [Core Writing Team. IPCC, Geneva, Switzerland, pp. 1–34. https://doi.org/10.59327/IPCC/AR6-9789291691647.001, 10.59327/IPCC/AR6-9789291691647.001.

Johnson, M.D., Klein, S.G., Lucey, N., Steckbauer, A., Shore, A., Camp, E.F., 2024. Editorial: drivers and consequences of ocean deoxygenation in tropical ecosystems. Front. Mar. Sci. 11, 1425902. https://doi.org/10.3389/fmars.2024.1425902.

Johnson, M.D., Scott, J.J., Leray, M., Lucey, N., Bravo, L.M.R., Wied, W.L., Altieri, A.H., 2021. Rapid ecosystem-scale consequences of acute deoxygenation on a Caribbean coral reef. Nat. Commun. 12. https://doi.org/10.1038/s41467-021-24777-3.

Kaelin, W.G., Ratcliffe, P.J., 2008. Oxygen sensing by metazoans: the central role of the HIF hydroxylase pathway. Mol. Cell 30, 393–402. https://doi.org/10.1016/j.molcel.2008.04.009.

Kassambara, A., 2023a. Rstatix: pipe-Friendly framework for basic statistical tests. R package version 0.7.2. https://rpkgs.datanovia.com/rstatix/.

Kassambara, A., 2023b. Ggpubr: "ggplot2" based publication ready plots. https://CRAN.R-project.org/package=ggpubr.

Kay, M., Elkin, L.A., Higgins, J.J., Wobbrock, J.O., 2021. mjskay/ARTool: ARTool 0.11.0. https://doi.org/10.5281/ZENODO.594511.

Keeling, R.F., Körtzinger, A., Gruber, N., 2010. Ocean deoxygenation in a warming world. Ann. Rev. Mar. Sci 2, 199–229. https://doi.org/10.1146/annurev.marine.010908.163855.

Lamarck, J.-B., 1816. Histoire naturelle des animaux sans vertèbres. Verdière, Paris. https://doi.org/10.5962/bhl.title.12712.

Leiva, F.P., Garcés, C., Verberk, W.C.E.P., Care, M., Paschke, K., Gebauer, P., 2018. Differences in the respiratory response to temperature and hypoxia across four life-stages of the intertidal porcelain crab Petrolisthes laevigatus. Marine Biology 165. https://doi.org/10.1007/s00227-018-3406-z.

Levin, L.A., 2018. Manifestation, drivers, and emergence of open ocean deoxygenation. Ann. Rev. Mar. Sci 10, 229–260. https://doi.org/10.1146/ANNUREV-MARINE-121916-063359.

Levin, L.A., Breitburg, D.L., 2015. Linking coasts and seas to address ocean deoxygenation. Nat. Clim. Change 5, 401–403. https://doi.org/10.1038/nclimate2595.

Love, M.L., Huber, W., Anders, S., 2014. Moderated estimation of fold change and dispersion for RNA-seq data with DESeq2. Genome Biol. 15. https://doi.org/10.1186/s13059-014-0550-8.

Maggioni, F., Pujo-Pay, M., Aucan, J., Cerrano, C., Calcinai, B., Payri, C., Benzoni, F., Letourneur, Y., Rodolfo-Metalpa, R., 2021. The bouraké semi-enclosed lagoon (New Caledonia) – a natural laboratory to study the lifelong adaptation of a coral reef ecosystem to extreme environmental conditions. Biogeosciences 18, 5117–5140. https://doi.org/10.5194/bg-18-5117-2021.

Majerová, E., Drury, C., 2022. Thermal preconditioning in a reef-building coral alleviates oxidative damage through a BI-1-mediated antioxidant response. Front. Mar. Sci. 9. https://doi.org/10.3389/fmars.2022.971332.

Mandic, M., Best, C., Perry, S.F., 2020. Loss of hypoxia-inducible factor 1α affects hypoxia tolerance in larval and adult zebrafish (Danio rerio). Proc. Biol. Sci. 287, 20200798. https://doi.org/10.1098/rspb.2020.0798.

Murphy, J.W.A., Richmond, R.H., 2016. Changes to coral health and metabolic activity under oxygen deprivation. PeerJ, e1956. https://doi.org/10.7717/PEERJ.1956/SUPP-1, 2016.

Nelson, H.R., Altieri, A.H., 2019. Oxygen: the universal currency on coral reefs. Coral Reefs 38, 177–198. https://doi.org/10.1007/s00338-019-01765-0.

Palumbi, S.R., Barshis, D.J., Traylor-Knowles, N., Bay, R.A., 2014. Mechanisms of reef coral resistance to future climate change. Science 344, 895–898. https://doi.org/10.1126/science.1251336.

Pezner, A.K., Courtney, T.A., Barkley, H.C., Chou, W.-C., Chu, H.-C., Clements, S.M., Cyronak, T., DeGrandpre, M.D., Kekuewa, S.A.H., Kline, D.I., Liang, Y.-B., Martz, T. R., Mitarai, S., Page, H.N., Rintoul, M.S., Smith, J.E., Soong, K., Takeshita, Y., Tresguerres, M., Wei, Y., Yates, K.K., Andersson, A.J., 2023. Increasing hypoxia on global coral reefs under ocean warming. Nat. Clim. Change 13 (4 13), 403–409. https://doi.org/10.1038/s41558-023-01619-2, 2023.

Pontes, E., Langdon, C., Al-Horani, F.A., 2023. Caribbean scleractinian corals exhibit highly variable tolerances to acute hypoxia. Front. Mar. Sci. 10, 861. https://doi.org/10.3389/FMARS.2023.1120262.

Qutub, A.A., Popel, A.S., 2008. Reactive oxygen species regulate hypoxia-inducible factor 1α differentially in cancer and ischemia. Mol. Cell Biol. 28, 5106–5119. https://doi.org/10.1128/MCB.00060-08.

R Core Team, 2021. R: a language and environment for statistical computing. https://www.R-project.org/.

Rabalais, N.N., Turner, R.E., Wiseman Jr., W.J., 2001. Hypoxia in the Gulf of Mexico. J. Environ. Qual. 30, 320–329. https://doi.org/10.2134/jeq2001.302320x.

Ritz, C., Baty, F., Streibig, J.C., Gerhard, D., 2015. Dose-response analysis using R. PLoS One 10, e0146021. https://doi.org/10.1371/journal.pone.0146021.

Röning, T., Magga, J., Laitakari, A., Halmetoja, R., Tapio, J., Dimova, E.Y., Szabo, Z., Rahtu-Korpela, L., Kemppi, A., Walkinshaw, G., Myllyharju, J., Kerkelä, R., Koivunen, P., Serpi, R., 2022. Activation of the hypoxia response pathway protects against age-induced cardiac hypertrophy. Journal of Molecular and Cellular Cardiology 164, 148–155. https://doi.org/10.1016/j.yjmcc.2021.12.003.

Roper, C.D., Suggett, D.J., Songsomboon, K., Edmondson, J., England, H., Haydon, T.D., Goyen, S., Duijser, C.M., Alderdice, R., Voolstra, C.R., Camp, E.F., 2025. Coral thermotolerance retained following year-long exposure to a novel environment. Sci. Adv. 11, eadu3858. https://doi.org/10.1126/sciadv.adu3858.

Ros, M., Suggett, D.J., Edmondson, J., Haydon, T., Hughes, D.J., Kim, M., Guagliardo, P., Bougoure, J., Pernice, M., Raina, J.B., Camp, E.F., 2021. Symbiont shuffling across environmental gradients aligns with changes in carbon uptake and translocation in the reef-building coral Pocillopora acuta. Coral Reefs 40, 595–607. https://doi.org/10.1007/s00338-021-02066-1.

Schoepf, V., Baumann, J.H., Barshis, D.J., Browne, N.K., Camp, E.F., Comeau, S., Cornwall, C.E., Guzmán, H.M., Riegl, B., Rodolfo-Metalpa, R., Sommer, B., 2023. Corals at the edge of environmental limits: a new conceptual framework to re-define marginal and extreme coral communities. Sci. Total Environ. 884, 163688. https://doi.org/10.1016/j.scitotenv.2023.163688.

Scucchia, F., Zaslansky, P., Boote, C., Doheny, A., Mass, T., Camp, E.F., 2023. The role and risks of selective adaptation in extreme coral habitats. Nat. Commun. 14, 4475. https://doi.org/10.1038/s41467-023-39651-7.

Seibel, B.A., Andres, A., Birk, M.A., Burns, A.L., Shaw, C.T., Timpe, A.W., Welsh, C.J., 2021. Oxygen supply capacity breathes new life into critical oxygen partial pressure (Pcrit). J. Exp. Biol. 224, jeb242210. https://doi.org/10.1242/jeb.242210.

Silbiger, N.J., Goodbody-Gringley, G., Bruno, J.F., Putnam, H.M., 2019. Comparative thermal performance of the reef-building coral Orbicella franksi at its latitudinal range limits. Marine Biology 166. https://doi.org/10.1007/S00227-019-3573-6.

Simancas-Giraldo, S.M., Xiang, N., Kennedy, M.M., Nafeh, R., Zelli, E., Wild, C., 2021. Photosynthesis and respiration of the soft coral Xenia umbellata respond to warming but not to organic carbon eutrophication. PeerJ 9, e11663. https://doi.org/10.7717/peerj.11663.

Solaini, G., Baracca, A., Lenaz, G., Sgarbi, G., 2010. Hypoxia and mitochondrial oxidative metabolism. Biochim. Biophys. Acta Bioenerg. 1797, 1171–1177. https://doi.org/10.1016/j.bbabio.2010.02.011, 16th European Bioenergetics Conference 2010.

Steckbauer, A., Duarte, C.M., Carstensen, J., Vaquer-Sunyer, R., Conley, D.J., 2011. Ecosystem impacts of hypoxia: thresholds of hypoxia and pathways to recovery. Environ. Res. Lett. 6, 025003. https://doi.org/10.1088/1748-9326/6/2/025003.

Stephens, T.G., Lee, J., Jeong, Y., Yoon, H.S., Putnam, H.M., Majerová, E., Bhattacharya, D., 2022. High-quality genome assembles from key Hawaiian coral species. GigaScience 11, giac098. https://doi.org/10.1093/gigascience/giac098.

Suggett, D.J., Nitschke, M.R., Hughes, D.J., Bartels, N., Camp, E.F., Dilernia, N., Edmondson, J., Fitzgerald, S., Grima, A., Sage, A., Warner, M.E., 2022. Toward bio-optical phenotyping of reef-forming corals using light-induced fluorescence transient-fast repetition rate fluorometry. Limnol Oceanogr. Methods 20, 172–191. https://doi.org/10.1002/lom3.10479.

Tremblay, N., Hünerlage, K., Werner, T., 2020. Hypoxia tolerance of 10 euphausiid species in relation to vertical temperature and oxygen gradients. Front. Physiol. 11. https://doi.org/10.3389/fphys.2020.00248.

Vaquer-Sunyer, R., Duarte, C.M., 2008. Thresholds of hypoxia for marine biodiversity. Proceedings of the National Academy of Sciences of the United States of America 105, 15452–15457. https://doi.org/10.1073/pnas.0803833105.

Veal, C.J., Carmi, M., Fine, M., Hoegh-Guldberg, O., 2010. Increasing the accuracy of surface area estimation using single wax dipping of coral fragments. Coral Reefs 29, 893–897. https://doi.org/10.1007/s00338-010-0647-9.

Voolstra, C.R., Buitrago-López, C., Perna, G., Cárdenas, A., Hume, B.C.C., Rädecker, N., Barshis, D.J., 2020. Standardized short-term acute heat stress assays resolve historical differences in coral thermotolerance across microhabitat reef sites. Glob. Change Biol. 26, 4328–4343. https://doi.org/10.1111/gcb.15148.

Wickham, H., 2016. ggplot2: Elegant Graphics for Data Analysis, second ed. Springer International Publishing. https://doi.org/10.1007/978-3-319-24277-4.

Wickham, H., François, R., Henry, L., Müller, K., Vaughan, D., 2023. Dplyr: a grammar of data manipulation. R package version 1.1.4. https://github.com/tidyverse/dplyr. https://dplyr.tidyverse.org.

Wobbrock, J.O., Findlater, L., Gergle, D., Higgins, J.J., 2011. The aligned rank transform for nonparametric factorial analyses using only anova procedures. In: Proceedings of the SIGCHI Conference on Human Factors in Computing Systems. Presented at the CHI '11: CHI Conference on Human Factors in Computing Systems. ACM, Vancouver BC Canada, pp. 143–146. https://doi.org/10.1145/1978942.1978963.

Zhang, Y., So, B.E., Farrell, A.P., 2021. Hypoxia performance curve: assess a whole-organism metabolic shift from a maximum aerobic capacity towards a glycolytic capacity in fish. Metabolites 11, 447. https://doi.org/10.3390/metabo11070447.